PAPER • OPEN ACCESS

Analysis of undulator and gyro-synchrotron radiation for application at tera-hertz

To cite this article: G. Mishra *et al* 2023 *J. Phys.: Conf. Ser.* **2484** 012013

Journal of Physics: Conference Series **2484** (2023) 012013 doi:10.1088/1742-6596/2484/1/012013

Analysis of undulator and gyro-synchrotron radiation for application at tera-hertz

G. Mishra[1], Mona Gehlot[2] and Vikesh Gupta[3]

[1] Laser and Insertion Device Application (LIDA) Laboratory, Devi Ahilya VishwaVidyalaya, Indore, India
[2] DESY, Hamburg, Germany
[3] Sushila Devi Bansal College of Engineering, Indore, India

E-mail: [1]gmishra_dauniv@yahoo.co.in, [3]vikesh@sdbc.ac.in

Abstract. We analyze the undulator and gyro -synchrotron radiation of the devices by equating the number of periods of the helical trajectory of the gyrating motion to the number of undulator periods. The gyro radiation is characterized by cyclotron resonance maser interaction exhibits superior line width quality but higher sensitive to beam energy spread when operated at tera-hertz due to finite larmor radius effects.

1. Introduction

Over the years the undulator technology have been renewed and upgraded enabling the free electron laser (FEL) [1-5] to be useful for different physics, chemistry, biology and engineering based applications. The bi-period, staggered array undulator, step tapered, Optical klystron undulators, Apple type and Delta undulators are examples of higher generation FEL schemes. On the other hand, electron cyclotron resonance masers (CRM) have been studied and developed in various schemes [6-10]. The Gyrotrons including Gyro-Klystrons, Gyro-TWTs, Gyro-BWO and Cyclotron Auto Resonance Masers (CARM) work on the principle of electron cyclotron resonance interactions.

Both the free electron laser and electron cyclotron resonance maser share important analogy and similarities [11-14]. The stimulated emission occurs in free electron laser due to ponderomotive wave causing axial micro bunching of electrons along the length of the undulator. The stimulated emission occurs in electron cyclotron maser due to azimuthal bunching of electrons due to relativistic cyclotron frequency. The free electron laser is tuned by varying either the electron beam energy or the undulator magnetic field strength. The wavelength of the electron cyclotron maser radiation is tuned by changing the electron beam energy or the axial magnetic field strength. In CRM, the resonance condition is given by $\omega = \omega_c + kc\beta_z$, ω, k are the electromagnetic wave angular frequency & axial wave number respectively. $\omega_c = eB_0 / \gamma m_e$ is the relativistic cyclotron frequency, B_0 is the axial magnetic field and e, m_e are the charge of electron and mass respectively. The resonance condition in the case of FEL reads $\omega = \omega_u + kc\beta_z$, ω_u is the undulator frequency. β_z is the longitudinal electron velocity. $\gamma = \left(1-\beta_z^2-\beta_x^2\right)^{-1/2}$ is the relativistic factor relating to the electron longitudinal velocity and electron transverse velocity. Substituting the expression for the longitudinal velocity, we get $\omega = 2\gamma^2\omega_u / 1 + K^2$ for the free electron laser and $\omega = 2\gamma\omega_c / 1 + \gamma^2\beta_\perp^2$ for the electron cyclotron maser. $K = 93B_1(T)\lambda_u(m)$ is the undulator parameter relating to the undulator field strength i.e B_1 and the period length of the undulator λ_u. $\beta_\perp$ is the initial electron transverse velocity of the gyrating electrons. The radiation frequency scaling with energy is linear i.e., $\omega \sim \gamma^1$ in the electron cyclotron resonance maser rather than squared i.e., $\omega \sim \gamma^2$ in free electron laser and to make the devices operate differently in tera hertz application [15-24].

In this paper we analyze the undulator radiation and gyro -synchrotron radiation by equating the period of the helical trajectory of the gyro device to the number of undulator periods. In section 2, the undulator radiation is reviewed. In section 3, the expression for the gyro synchrotron radiation is derived and compared. In section 4, results of the analysis are discussed. The effects of the beam energy spread is included in both the devices. It is shown that the gyro device yields comparable photons per second per mrad^2 per 1% bandwidth with undulator based device but with higher sensitive in beam energy spread.

2. Undulator radiation

The field of an undulator is denoted as,

$$\vec{B} = \left[0, \{B_1 \sin(k_u z)\}\,\hat{y}, 0\right] \tag{1}$$

Where λ_u is the undulator period with $k_u = 2\pi/\lambda_u$. $\omega_u = c\,k_u$. B_1 is the field amplitudes. Using Lorentz force equation we get,

$$\beta_x = -\frac{K}{\gamma}\left[\cos\left(k_u z\right)\right] + \theta_x \tag{2}$$

Where $K = eB_1 / m_e c k_u$ is an undulator parameter. Eq. (2) assumes imperfect trajectory with angular incidence. Further the longitudinal electron velocity as,

$$\beta_z = \beta^* - \frac{K^2}{4\gamma^2}\left[\cos\left(2\omega_u t\right)\right] + \frac{K\,\theta_x}{\gamma}\left[\cos\left(\omega_u t\right)\right] \tag{3}$$

$$\beta^* = 1 - \frac{1}{2\gamma^2}\left\{1 + \frac{K^2}{2} + \gamma^2\theta_x^2\right\}$$

From [2,3], the transverse and the longitudinal electron trajectory is written as,

$$x = -\frac{cK}{\gamma\omega_{u1}}\left[\sin\left(\omega_u t\right)\right]$$

$$z = \beta^* ct - \frac{cK^2}{8\gamma^2\omega_u}\left[\sin 2\omega_u t\right] + \frac{c\theta_x K}{\gamma\omega_u}\left[\sin\omega_u t\right] \tag{4}$$

The brightness is calculated with the help of the Lienard-Weichert integral,

$$\frac{d^2 I}{d\omega d\Omega} = \frac{e^2\omega^2}{16\pi^3\varepsilon_0 c}\left|\int_{-\infty}^{+\infty}\left\{\hat{n}\times(\hat{n}\times\vec{\beta})\right\}\exp\left[i\omega\left(t - \frac{z}{c}\right)\right]dt\right|^2 \tag{5}$$

where,

$$\hat{n}\times(\hat{n}\times\vec{\beta})\Big|_x = \frac{K}{\gamma}\left[\cos\left(k_u z\right)\right]-\theta_x \tag{6}$$

The exponential in Eq. (5) reads

$$\begin{gathered}\exp\left[i\omega\left(t-\frac{z}{c}\right)\right]=\sum_m J_m\left(\xi_1,\xi_2\right)\exp\left(i\nu_u t\right)\\ \xi_1=\frac{\omega\theta_x K}{\gamma\omega_u},\xi_2=-\frac{\omega K^2}{8\gamma^2\omega_u}\end{gathered} \tag{7}$$

The detuning parameter ν is given by

$$\nu_u=\omega_u\left[\frac{\omega}{2\gamma^2\omega_u}(1+K^2/2+\gamma^2\theta_x^2)-m\right] \tag{8}$$

Where $J_m\left(\xi_1,\xi_2\right)$ is the Generalized Bessel Functions (GBF)[25]. Using the expressions from above, we get,

$$\frac{d^2I}{d\omega d\Omega}=\sum\nolimits_m \frac{e^2\omega^2T^2}{64\pi^3\varepsilon_0 c\gamma^2}[JJ]_u^{\,2}\frac{\sin^2(\nu_u T/2)}{(\nu_u T/2)^2} \tag{9}$$

Where, $[JJ]_u$ reads as,

$$[JJ]_u=\left\{J_{m+1}\left(\xi_1,\xi_2\right)+J_{m-1}\left(\xi_1,\xi_2\right)\right\}-(2\gamma\theta_x/K)J_m\left(\xi_1,\xi_2\right) \tag{10}$$

The resonance condition i.e. $\nu_u=0$ is obtained as,

$$\omega=2\gamma^2 m\omega_u/(1+K^2/2+\gamma^2\theta_x^2) \tag{11}$$

The angular energy distribution function is [26],

$$F_m(K,\gamma\theta_x)=m^2[JJ]_u^2\frac{K^2}{\left(1+K^2/2+\gamma^2\theta_x^2\right)^2} \tag{12}$$

We rewrite Eq. (9) as

$$\frac{d^2I}{d\omega d\Omega}=\sum\nolimits_m \frac{e^2\gamma^2N_u^2}{4\pi\varepsilon_0 c}\frac{K^2}{\left(1+K^2/2+\gamma^2\theta_x^2\right)^2}m^2[JJ]_u^2\frac{\sin^2(\nu_u T/2)}{(\nu_u T/2)^2} \tag{13}$$

If the number of photons radiated per second with energy $h\omega/2\pi$ is $\dot{N}$ then the power radiated is $P=\dot{N}h\omega/2\pi$. The result when calculated in terms of $d\omega/\omega$ read as ,

$$\frac{d^2\dot{N}}{d\Omega\, d\omega/\omega}=\sum\nolimits_m \frac{e^2\gamma^2N_u^2}{4\pi\varepsilon_0 c}\frac{I_b}{e}\frac{2\pi}{h}\frac{K^2}{\left(1+K^2/2+\gamma^2\theta_x^2\right)^2}m^2[JJ]_u^2\frac{\sin^2(\nu_u T/2)}{(\nu_u T/2)^2} \tag{14}$$

Where, I_b =beam current, in units of photons per second per mrad^2 per 0.1% bandwidth, we get

$$\frac{d\dot{N}}{d\Omega}=1.74\times10^{14}\sum\nolimits_m N_u^2E^2I_b\frac{K^2}{\left(1+K^2/2+\gamma^2\theta_x^2\right)^2}m^2[JJ]_u^2\frac{\sin^2(\nu_u T/2)}{(\nu_u T/2)^2} \tag{15}$$

Eq. (15) is valid for a monoenergetic electron beam, A beam characterized by a finite spread in beam energy induce shift in the resonance frequency and radiation emitted at a given harmonic. From Eq. (11) we read, $\Delta\omega/\omega=2\Delta\gamma/\gamma$. Assuming that the beam has a Gaussian energy distribution in beam energy spread with r.m.s value σ_ε , $f(\varepsilon)=\frac{1}{\sqrt{2\pi}\sigma_\varepsilon}\exp\left(\frac{-\varepsilon}{2\sigma_\varepsilon^2}\right)$ we find $\nu\to\nu_0+\delta\nu_\varepsilon$,

$\delta\nu_\varepsilon = 4N_u\pi\varepsilon$, $\varepsilon = (\gamma-\gamma_0)/\gamma_0$, γ_0 is the resonant energy for which $\nu_0 = 0$. After a handful of algebraic steps ,we get from Eq.[15]

$$\frac{d\dot{N}}{d\Omega} = 1.74\times10^{14}\sum_m N_u^2 E^2 I_b F_m(K,\gamma\theta_x) f(\nu_u,\sigma_\varepsilon) \tag{16}$$

where $$f(\nu_u,\sigma_\varepsilon) = 2\int_0^1 dt(1-t)\cos(\nu_0 t)\exp\left(\frac{-16\pi^2 N_u^2\sigma_\varepsilon^2 t^2}{2}\right)$$

3. Gyro-synchrotron radiation

In an axial magnetic field, the electron velocity and trajectories are

$$\beta_x = -\beta_\perp\cos(\varpi_c t)+\theta_x$$
$$\beta_y = \beta_\perp\sin(\varpi_c t) \tag{17}$$

Where, $\varpi_c = eB_0/m_e\gamma$. $\omega_c = eB_0/m_e$. We get the longitudinal component as,

$$\beta_z = \beta^* + \theta_x\beta_\perp\cos\varpi_c t \qquad ,\beta^* = 1-\frac{1}{2\gamma^2}\left\{1+\gamma^2\beta_\perp^2+\gamma^2\theta_x^2\right\}$$

and the electron trajectories as,

$$x = -\frac{c\beta_\perp}{\varpi_c}\sin(\varpi_c t) \quad ,y = -\frac{c\beta_\perp}{\varpi_c}\cos(\varpi_c t) \quad z = c\beta^* t + (\theta_x c\beta_\perp/\varpi_c)\sin\varpi_c t \tag{18}$$

The triple vector products are evaluated as,

$$\left(\hat{n}\times(\hat{n}\times\vec{\beta})\right)_x = \beta_\perp\cos(\varpi_c t)-\theta_x$$
$$\left(\hat{n}\times(\hat{n}\times\vec{\beta})\right)_y = -\beta_\perp\sin(\varpi_c t)$$
$$\frac{\hat{n}.\vec{r}}{c} = -\frac{\theta_x\beta_\perp}{\varpi_c}\sin(\varpi_c t)+\beta^* t$$
$$\exp\left[-i\xi_3\sin\varpi_c t\right] = \sum_n J_n(\xi_3,0)\exp(-in\varpi_c t) \qquad ,\xi_3 = \omega\theta_x\beta_\perp/\varpi_c \tag{19}$$

For the exponential We get, $$\exp\left[i\omega\left(t-\frac{z}{c}\right)\right] = \sum_n J_n(\xi_3,0)\exp(i\nu_c t) \tag{20}$$

The detuning parameter is defined as,

$$\nu_c = \varpi_c\left[\frac{\omega}{2\gamma^2\varpi_c}\left(1+\gamma^2\beta_\perp^2+\gamma^2\theta_x^2\right)-n\right], \tag{21}$$

Using the earlier equations, we get Eq. (5) as,

$$\frac{d^2I}{d\omega d\Omega} = \sum_n \frac{e^2\omega^2T^2\beta_\perp^2}{64\pi^3\varepsilon_0 c} n^2[JJ]_c^2 \frac{\sin^2(\nu_c T/2)}{(\nu_c T/2)^2} \tag{22}$$

$$[JJ]_c = a_0 + ia_1 \quad ,a_0 = \left\{J_{n+1}(\xi_3,0)+J_{n-1}(\xi_3,0)\right\} - 2(\gamma\theta_x/\gamma\beta_\perp)J_n(\xi_3,0)$$

$a_1 = \left\{J_{n+1}(\xi_3,0)-J_{n-1}(\xi_3,0)\right\}$ where $\xi_3 = 2\gamma\theta_x\gamma\beta_\perp/1+\gamma^2\beta_\perp^2+\gamma^2\theta_x^2$. We re-write Eq.22 as,

$$\frac{d^2I}{d\omega d\Omega} = \sum_n \frac{e^2\gamma^2(\varpi_c T)^2}{4\pi\varepsilon_0 c}\frac{\gamma^2\beta_\perp^2}{(1+\gamma^2\beta_\perp^2+\gamma^2\theta_x^2)^2} n^2[JJ]_c^2 \frac{\sin^2(\nu_c T/2)}{(\nu_c T/2)^2} \tag{23}$$

Eq. (23) is further simplified to

$$\frac{d\dot{N}}{d\Omega}=1.74\times10^{14}\sum_n N_c^2E^2I_b\frac{\beta_\perp^2}{(1+\gamma^2\beta_\perp^2+\gamma^2\theta_x^2)^2}n^2[JJ]_c^2\frac{\sin^2(\nu_cT/2)}{(\nu_cT/2)^2} \tag{24}$$

where $\omega_c=2\pi c/\Lambda_c$, $N_c\Lambda_c$ is the total interaction length. The angular energy function is calculated as,

$$F_n(\beta_\perp,\gamma\theta_x)=\frac{\beta_\perp^2}{(1+\gamma^2\beta_\perp^2+\gamma^2\theta_x^2)^2}n^2[JJ]_c^2 \tag{25}$$

Eq. (25) alternately can be defined as,

$$F_n(\gamma\beta_\perp,\gamma\theta_x)=\frac{\gamma^2\beta_\perp^2}{(1+\gamma^2\beta_\perp^2+\gamma^2\theta_x^2)^2}n^2[JJ]_c^2$$

Eq. (24) is valid for a monoenergetic electron beam, A beam characterized by a finite spread in beam energy induce shift in the resonance frequency and radiation emitted at a given harmonic. From Eq. (11) we read, $\Delta\omega/\omega=\Delta\gamma/\gamma$. Assuming that the beam has a Gaussian energy distribution in beam energy spread with r.m.s value σ_ε , $f(\varepsilon)=\frac{1}{\sqrt{2\pi\sigma_\varepsilon}}\exp\left(\frac{-\varepsilon}{2\sigma_\varepsilon^2}\right)$ we find $\nu\rightarrow\nu_0+\delta\nu_\varepsilon$, $\delta\nu_\varepsilon=2N_c\pi\varepsilon$, $\varepsilon=(\gamma-\gamma_0)/\gamma_0$, γ_0 is the resonant energy for which $\nu_0=0$.

$$\frac{d\dot{N}}{d\Omega}=1.74\times10^{14}\sum_n N_c^2E^2I_bF_n(\beta_\perp,\gamma\theta_x)f(\nu_c,\sigma_\varepsilon)$$

Where

$$f(\nu_c,\sigma_\varepsilon)=2\int_0^1 dt(1-t)\cos(\nu_0t)\exp(\frac{-16\pi^2N_c^2\sigma_\varepsilon^2t^2}{8}) \tag{26}$$

4. Results and discussion

In this paper, we discuss the theory of synchrotron radiation in undulator magnet and compare its characteristics to gyro synchrotron radiation. The electron in the axial magnetic field executes helical trajectories and emits synchrotron radiation at cyclotron resonance frequency. The comparison is based on equating the number of turns in the helical trajectory to the number of undulator periods in the calculations for photons per second per mrad2 per 0.1% BW. The undulator parameters are $\gamma=19.45$ $B_1=0.62T$, $K=2.883$, $N_u=100$, $\lambda_u=0.05m$. The calculations in the paper are done with beam current of 0.3 A. The radiation frequency at these parameters calculates to $f=880GHz$. The angular energy distribution function for the undulator magnet is given in Eq. (12) and is plotted in Figure1.The peak value of this function decreases for higher values of imperfect entry of the electron to the undulator magnet. At $\gamma\theta_x=0{,}0.1{,}0.5$, the distribution function goes down to 0.36 and 0.15 from 0.38. This amounts to a drop of 5 % and 60 % respectively. The $\gamma\theta_x=0.5$ corresponds to 1.5 degree of angular imperfection in the entry of the electron along the undulator magnet. A drop in the value of the distribution function indicates a drop in the photon number. In Figure 2, the effects of beam energy spread on the undulator radiation is shown. A finite beam is characterized by finite energy spread and in our calculation the drop in intensity is about 12 % for $\sigma_e=0.1\%$. Figure 3 and Figure 4 is plotted for a quantitative evaluation of photons per second per mrad^2 per 0.1% BW at different beam energy spread and angular injection angle of the electron to the undulator magnet.

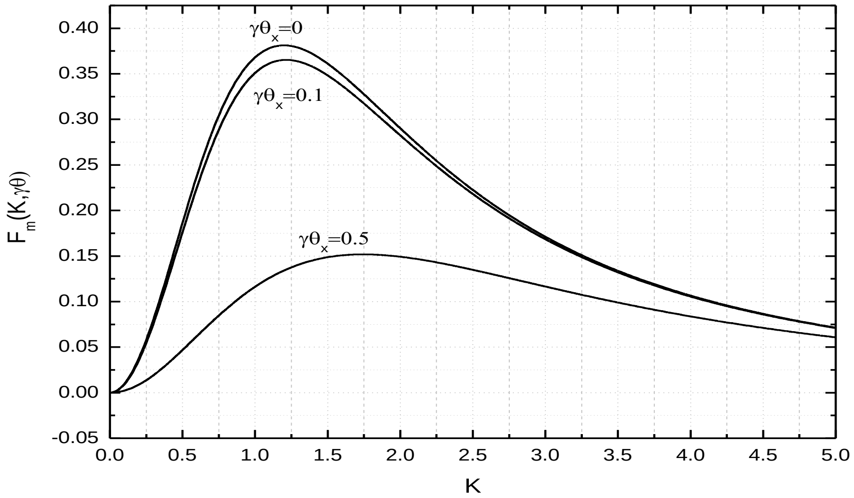

Figure 1. Angular energy distribution function of undulator radiation

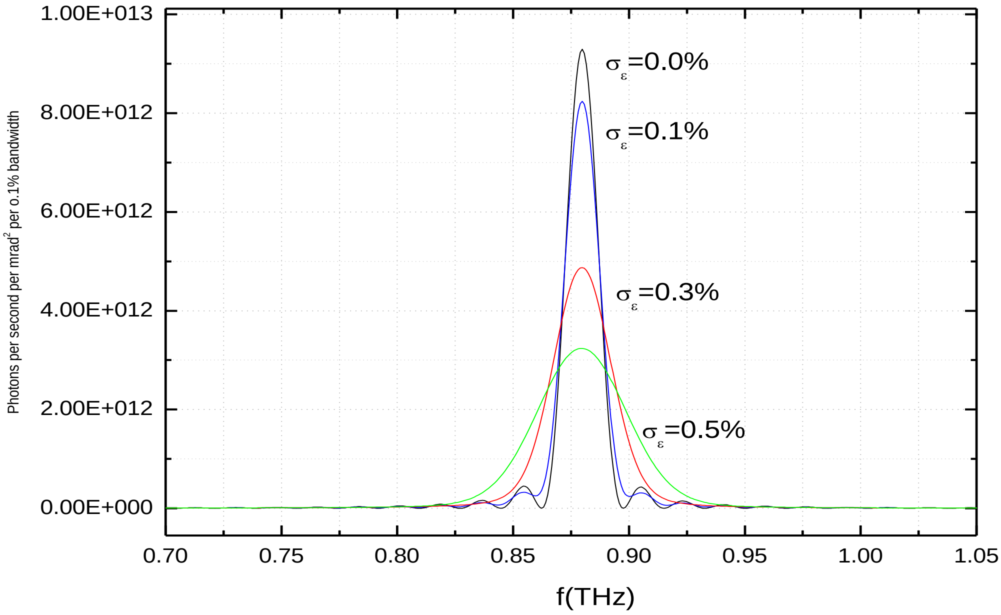

Figure 2. Effects of beam energy spread on photons per second per mrad^2 per 0.1% BW

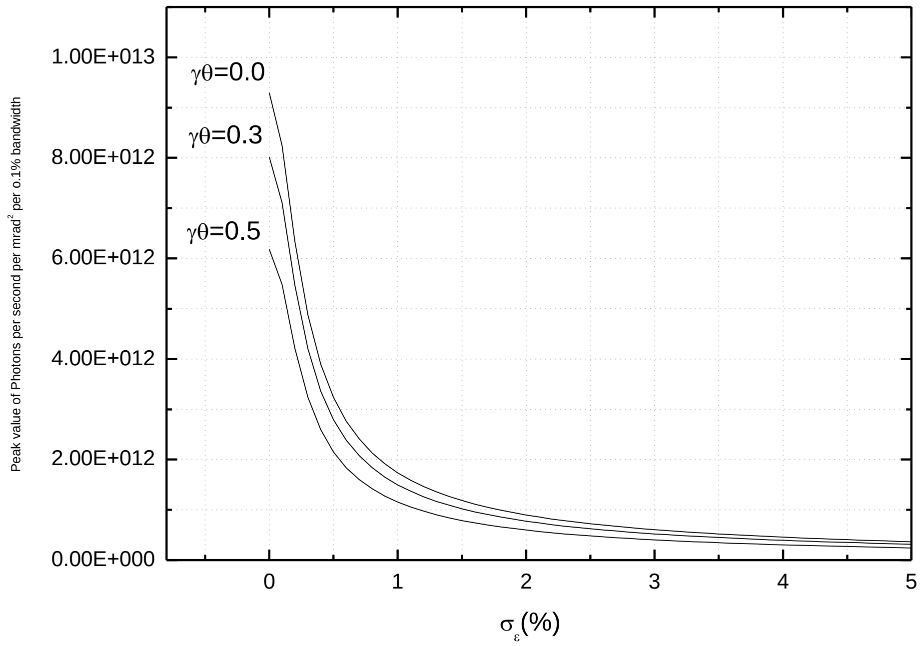

Figure 3. Effects of beam energy spread

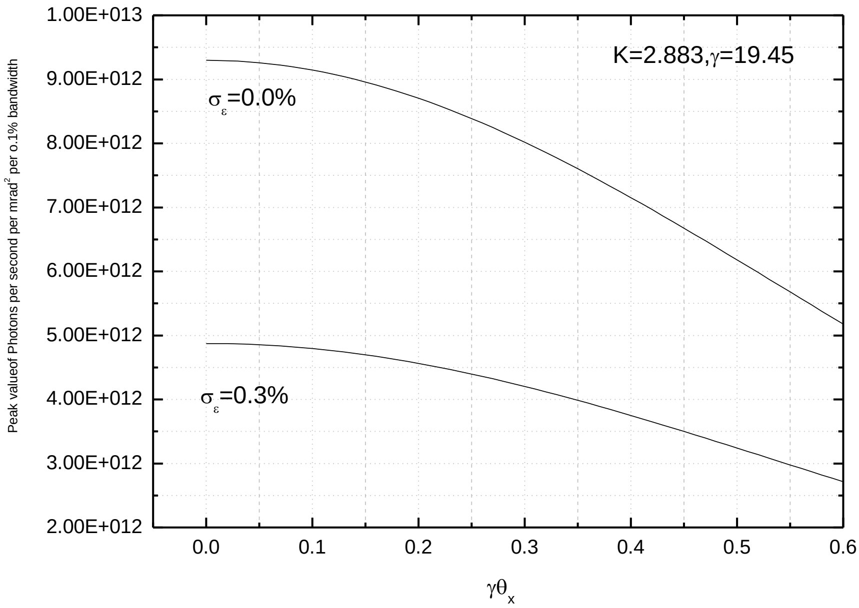

Figure 4. Effects of beam energy spread

Eq. (25) defines the angular distribution function of the gyro synchrotron radiation and is plotted in Figure 5a and Figure 5b. The function recommends peak value at $\beta_{\perp} = 0.1$. The radiation wavelength is fixed 880GHz and equivalent parameter of the gyro synchrotron radiation is calculated

Journal of Physics: Conference Series **2484** (2023) 012013 doi:10.1088/1742-6596/2484/1/012013

from $\gamma\beta_\perp = 1$ (Figure 5b). The radiation frequency reads from Eq. (21) and is given by $f = 28\gamma B$ GHz. For parameters of $\beta_\perp = 0.06$ $\gamma = 16.66, B_0 = 1.88T, f = 880$ GHz , Figure 6 plots photons per second per mrad^2 per 0.1% BW for various values of the beam parameter. By increasing the value of $\beta_\perp$, the value is increased. The quantity $\beta_\perp$ defines the larmor orbit of the electron i.e $r_L = c\beta_\perp / \omega_c$ .In practical units, using $f_c = 28B$ GHz we get $r_L = 1.7\times10^{-3}\beta_\perp / B$. For $\beta_\perp = 0.06$ $B_0 = 1.88T$, the larmor orbit is 54 micron. The larmor orbit is kept at this value in this paper. By decreasing the value of $\beta_\perp$, the value of the magnetic field requirement is lowered in order that the larmor orbit is kept constant at this value. The photons per second per mrad^2 per 0.1% BW is plotted for several values of $\beta_\perp$ in Figure 6. The corresponding magnetic field requirement is computed from the larmor orbit of 54 micron. At higher $\beta_\perp$, the intensity is increased can be made comparable to undulator radiation as the radiation is directly proportional to the cyclotron frequency. Higher value of the cyclotron frequency is auto-compulsion in the case as larmor orbit is kept constant. The effect of beam energy spread is studied in Figure 7. The effects of beam energy spread is severe on gyro synchrotron radiation as beam energy spread of 0.1% drops the photons per second per mrad^2 per 0.1% BW by 60%. The reason for this drastic fall is obvious due to following reasons. In order to get a comparable analysis, it is required to keep the interaction length equal. Thus, we are led to $N_c\Lambda_c = N_u\lambda_u$ where N_c, Λ_c are the number of turns in the helical trajectory and period of the helical trajectory. $N_{u,}\lambda_u$ are the undulator number of period and period length respectively $\Lambda_c = 2\pi c / \omega_c$. For stronger magnetic field Λ_c is smaller, hence N_c is higher. For $\beta_\perp$ values of 0.05, 0.06, N_c is 733 and 880 respectively Λ_c is 6.8 mm and 5.6 mm respectively. Thus, for an undulator length of 50 mm period and 100 periods, the Gyro synchrotron device works as a short period and higher number of period device. This equivalence makes the gyro synchrotron device with comparable intensity with undulator based device but with higher sensitive to beam energy spread.

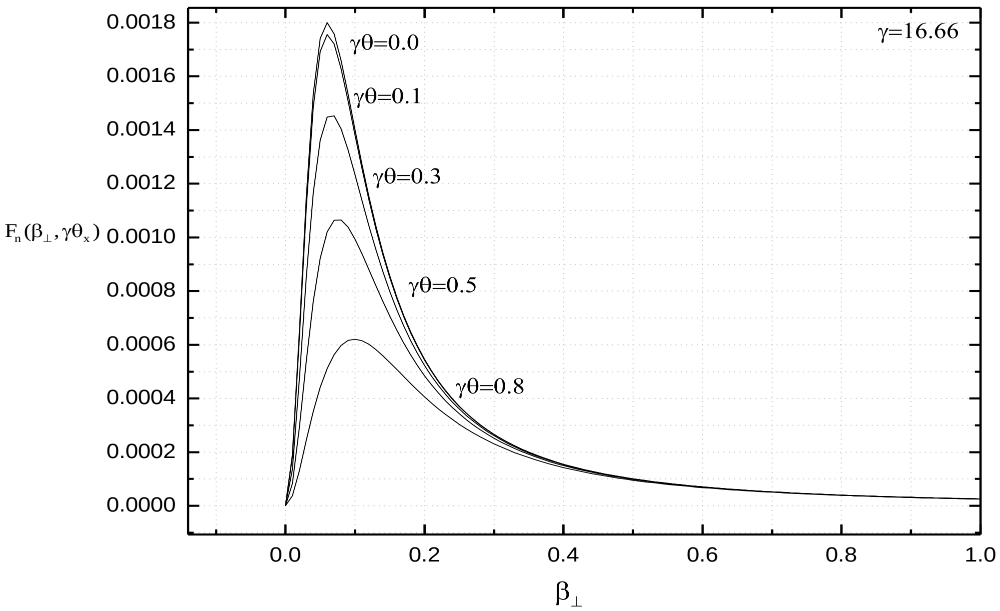

Figure 5a. Angular energy distribution function for the gyro radiation

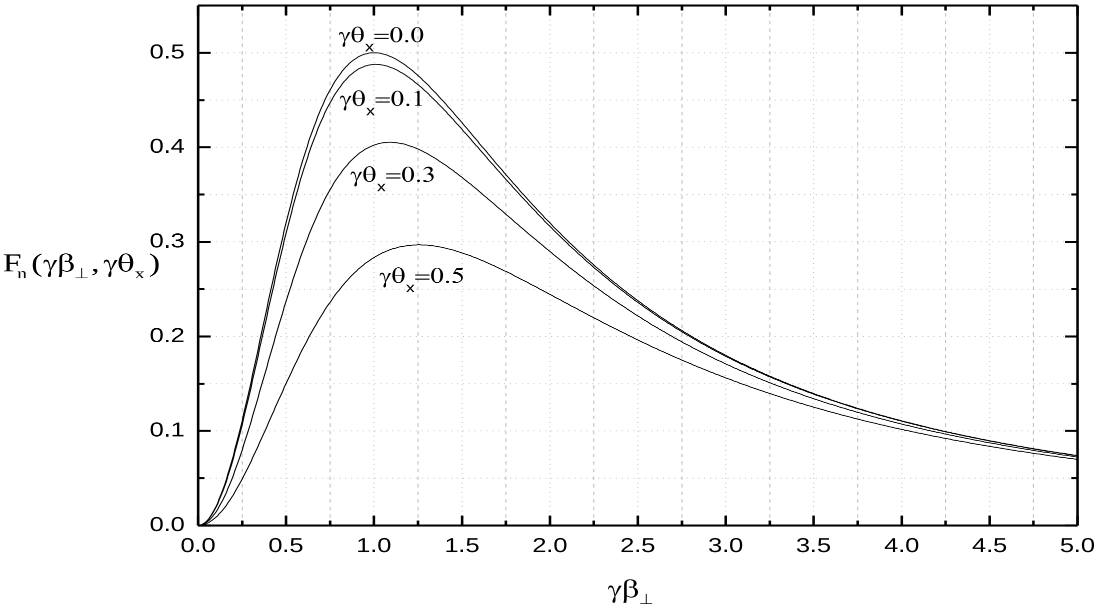

Figure 5b. Angular energy distribution function for the gyro radiation

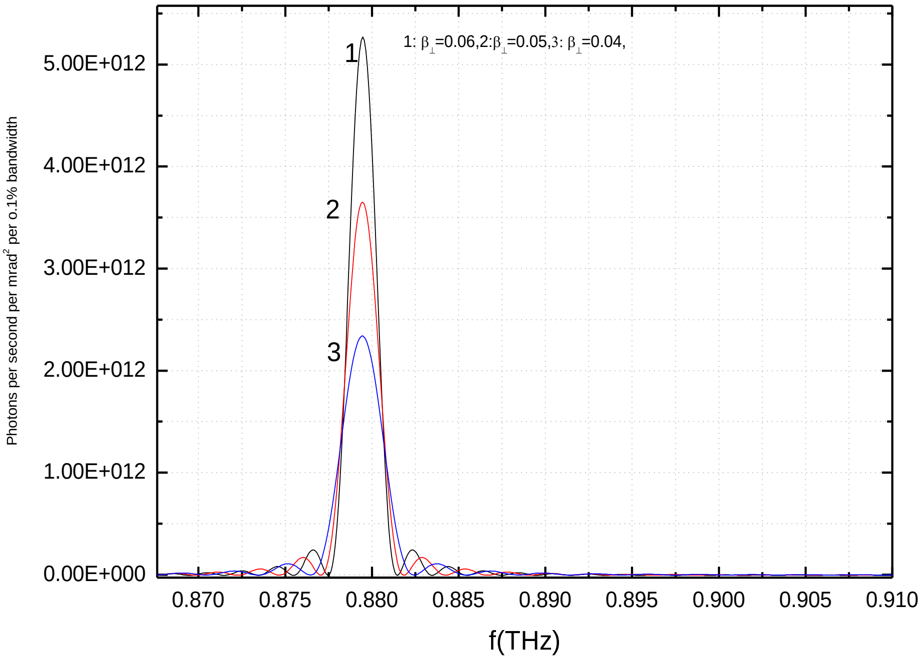

Figure 6. Gyro-synchrotron radiation frequency

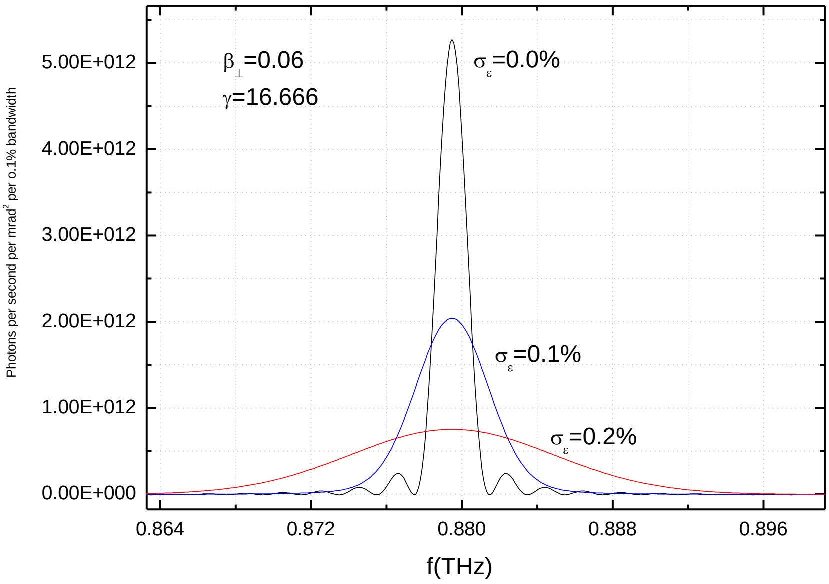

Figure 7. Effects of beam energy spread on gyro radiation

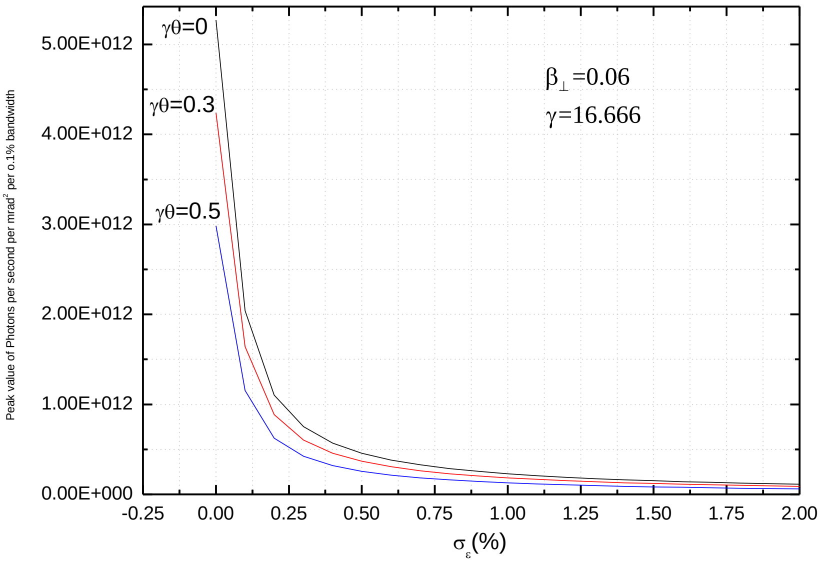

Figure 8. Effects of beam energy spread and angular injection

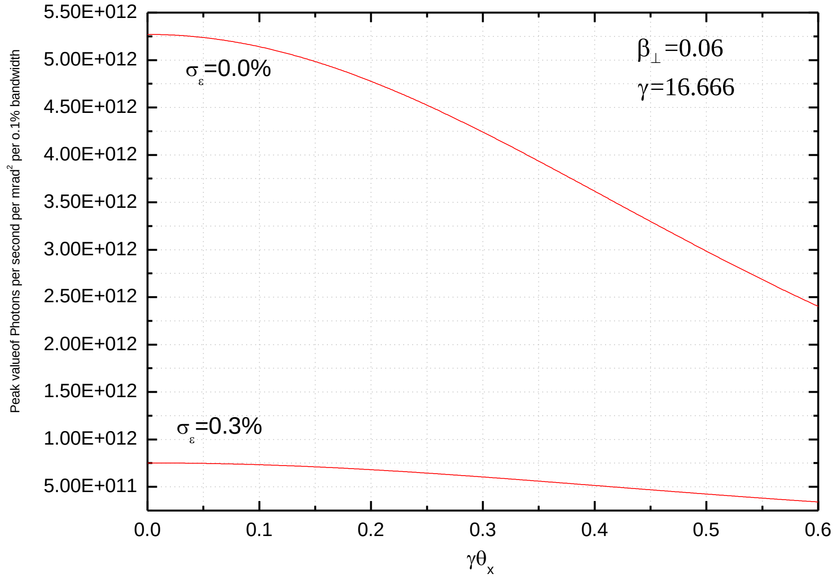

Figure 9. Effects of beam energy spread

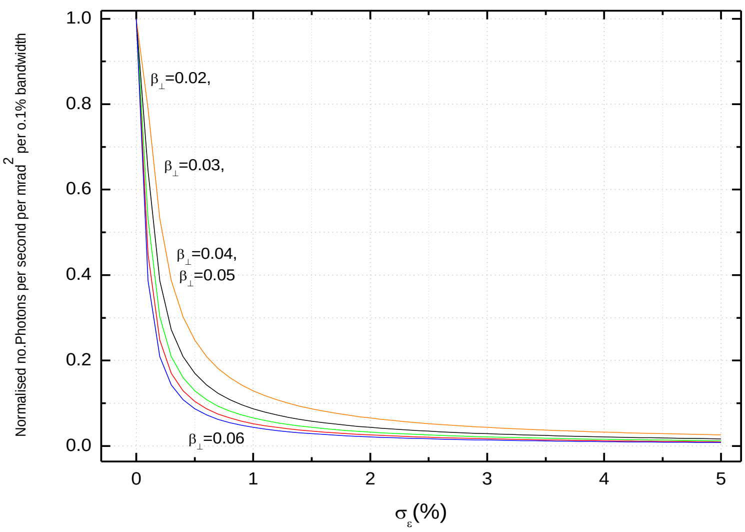

Figure 10. Effects of beam energy spread with different $\beta_\perp$

A quantitative evaluation of the beam energy spread with angular effects is given in Figure 8 and Figure 9 respectively. A higher value $\beta_\perp$ is accompanied by higher intensity and carries higher sensitive to beam energy spread due to short period length and higher number of turns as seen in Figure 10. In Figure 11 both the undulator radiation and the gyro radiation are compared. The gyro radiation is superior in terms of the line width over the undulator radiation. The line width of radiation is inversely proportional to the number of periods in undulator based devices. In the calculation the undulator period length is $\lambda_u = 0.05m$ and number of undulator period is $N_u = 100$. In the case with finite $\beta_\perp$,the period is calculated from $\Lambda_c = 2\pi c / \omega_c$. A stronger axial field results in shorter period in comparison to the undulator period, hence more number of periods for the same interaction length and the radiation exhibits good line width behavior shown in Figure 11. In Figure 12 we show the effects of beam energy spread for perfect beam. The gyro radiation has a sharp fall. For a perfect beam the gyro radiation and undulator radiation exhibit less sensitive as compared to imperfect entry, however at large values this effect is substantially large (Figure 13).

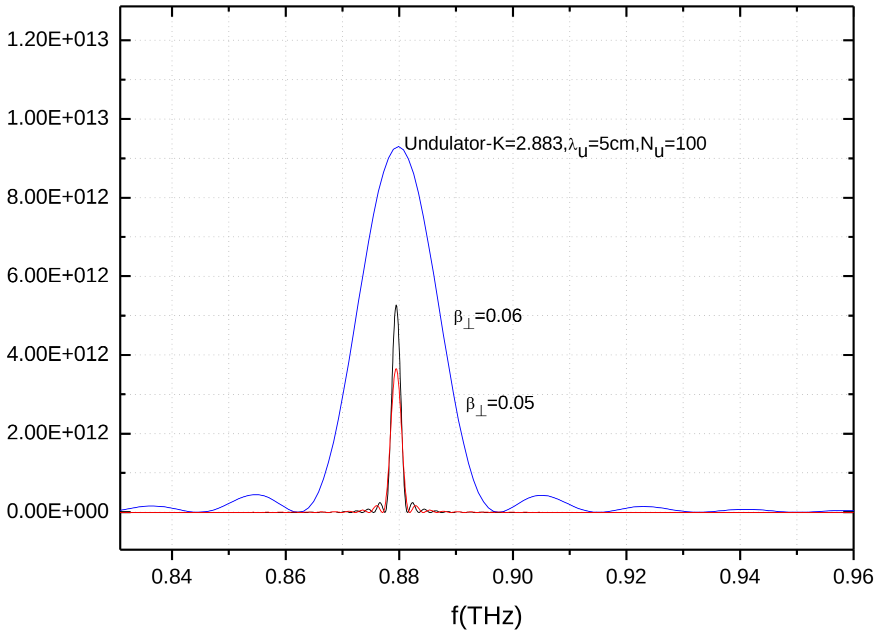

Figure 11. Line width comparison undulator radiation and gyro radiation

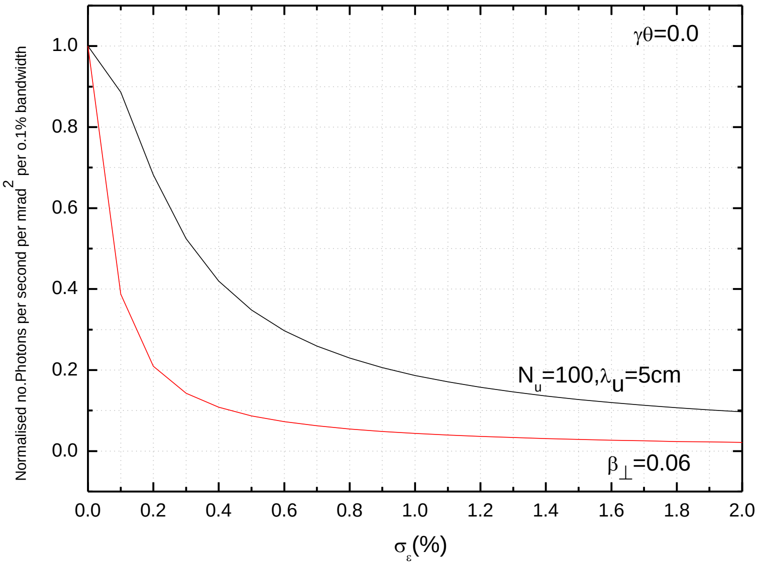

Figure 12. Effects of beam energy spread: undulator and gyro device

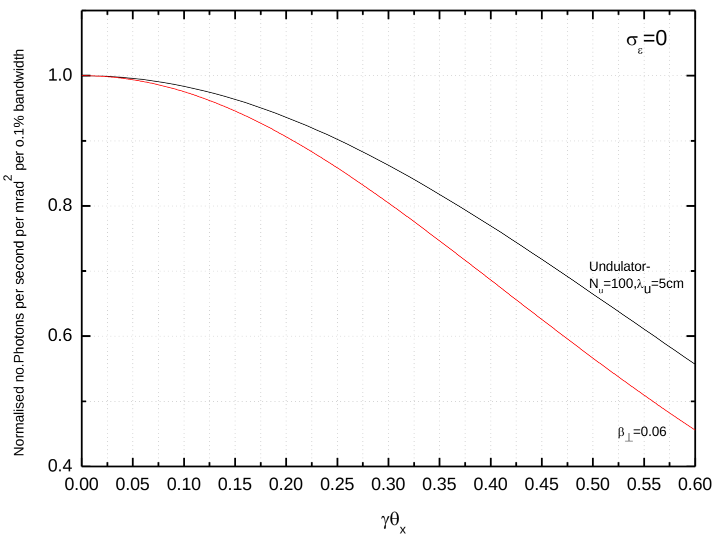

Figure 13. Effects of an angle on undulator and gyro device

In conclusion, the undulator radiation and gyro synchrotron radiation is analyzed with a number of equivalent parameters. The gyro radiation characterized by cyclotron resonance maser interaction exhibits superior line width quality but higher sensitive to beam energy spread when operated at tera hertz.

Acknowledgment
The work has been carried out by a financial grant from Science and Engineering Research Board (SERB) ,Delhi Government of India through a Core Research Grant i.e CRG/2022/001007.

The author Dr. Vikesh Gupta wish to express his gratitude to the organizers for awarding the paper as best research paper and awarding him for the best presentation at the conference.

References

[1] Dattoli G, Palma E D, Pagnutti S and Sabia E 2018 Free electron coherent sources: from microwave to X–rays, *Physics Reports*,**739**, pp. 1-51.
[2] Seddon E A, Clarke J A, Dunning D J, Masciorecchio C, Miline C J, Parmigiani F, et al 2017 Short wavelength free electron laser sources and science: a review, Reports on Progress in Physics, 80, No.11.
[3] Pellegrini C 2016 X-ray free electron lasers: from dreams to reality physica Scripta, No. T169, 014004.
[4] Rossbcch J, Schneider J R and Wurth W 2019 10 years of Pioneering x-ray science at the free electron laser FLASH at DESY Physics Reports, 808, pp. 1-74.
[5] Tanaka T 2017 Current status and future prospective of accelerator-based x-ray light source: Journal of Optics, 19, No.9.
[6] Chu K R 2004 The electron cyclotron resonance maser, Rev.Modern Physics, 76, pp. 489.
[7] McNeil B W J, Gordon R M Robb and Phelps A D R 1997 A Self-consistent single particle theory of the cyclotron resonance maser, Journal of Physics D: Applied Physics, 30, No.11.
[8] Symons R S, Jory H R, 1981 Cyclotron resonant Devices, Advances in Electronics and electron Physics, 55, 1-75.
[9] Cole N, Antonsen T M, 2017 Electron cyclotron resonance gain in the presence of collisions, IEEE Transactions on plasma science, 45, No.11.
[10] Wang C, 1988 Small signal analysis of a free electron cyclotron resonance laser, Phy. Rev A, 38, No.12, pp. 6215.
[11] Thumm M, 2017 State of the art of high power Gyro-devices and free electron masers, KIT scientific Reports, 7750.
[12] Palma E D, Sabia E, Dattoli G, Licciardi S, 2017 Cyclotron auto resonance maser and free electron laser devices: a unified point of view, Journal of Plasma Physics, 83, No.1.
[13] Kho T H, Lin A T, 1988 Combined wiggler and solenoidal field effects in free electron laser and electron cyclotron maser, Int Journal of Electronics, 65, No.3.
[14] Dattoli G, Palma E D, Doria A, ,Sabia E, Spassovsky I, SCeccuzzi S, Tuccillo A, 2014 The Gyrotron CARM and FEL devices: An analytical unified formulation for the small signal analysis, Tenth International Vacuum electron source conference (IVESC) , S . Petersburg, Russia.
[15] Vinokurov N, 2011 Free electron lasers as a high power tera hertz sources, Journal of Infrared and millimeter and tera hertz waves, New York, 32, No.11, 1123-1143.
[16] Booske John H, Dobbs R J, Joya S D, Kory C L, Neil G R, Park G S, Park J, Temkin R J, 2011 Vacuum electronic high power tera hertz sources, IEEE Transaction on tera hertz science and technology ,1,No.1, 54.
[17] Vinokurov N A, 2018 Generating high power tera hertz and far infrared electromagnetic radiation with relativistic electrons, EPJ Web of conferences,TERA-2018, 195,00004.
[18] Idehara T, Sabchevski S P, Glyavin M, Mitsundo S, 2020 The gyrotrons as promising radiation sources for Tera Hertz sensing and imaging, Applied Sciences, 10,No.3, 980.
[19] Qi X, Du C, Liu Shi Pan, 2017 Tera Hertz Broadband tunable pulse gyrotron, Scientica Sinica Informationis, 47, No.12, pp. 1741.
[20] Kao S H, Chiu C C, Pao K F, Chu K R, 2011 Competition between harmonic cyclotron maser Interactions in the tera hertz regime, Phys Rev. Lett, 107, 135101.
[21] Pan Shi, Chao Hai Du, Xiang-Bo Qi, Pu-Kun Liu, 2017 Broadband tera Hertz power extracting by using electron cyclotron maser, Scientific Reports, 7, Artcle No.7265.
[22] Li C D, Kao S H, Chang P C, Chu K R, 2015 Tera Hertz electron cyclotron maser interactions with on axis encircling electron beam, Phys of Plasmas, 22, 043109.

[23] Du C H, X-Bo Qi ,L-Bo Kong, Pu-Kun Liu, Zheng-Di Li, S.X. Xu, Zhi-Hui Geng, Liu Xiao, 2014 Broadband tunable pre bunched electron cyclotron maser for tera Hertz applications, IEEE Transactions on tera Hertz science and Technology, 5, 2.
[24] Bratman V, Lurie Yuri, Opariva Yu Liya, Savilov A, 2019 Capabilities of tera hertz cyclotron and undulator radiation from short ultra relativistic electron bunches, Instruments, MDPI, 3,55.
[25] Dattoli G, Renieri A, Torre E, 1993 Lectures on free electron theory and related topics, World Scientific.
[26] Clarke J, 2004 The Science & Technology of Undulators, Oxford University Press.